interactions and enzyme quaternary structure, and exploration of evolutionary relationships (*20*, *21*). We have, in essence, caught evolution in the act of adding an iron sulfur cluster to thioredoxin, enabling it to act as a thiol oxidant. Our results show that the acquisition of cofactors is evolutionarily a rather simple process, and our ability to generate an artificial pathway for oxidative protein folding highlights the plasticity of redox metabolism.

References and Notes

1. C. S. Sevier, C. A. Kaiser, *Nature Rev. Mol. Cell Biol.* **3**, 836 (2002).
2. J. F. Collet, J. C. A. Bardwell, *Mol. Microbiol.* **44**, 1 (2002).
3. P. H. Bessette, F. Aslund, J. Beckwith, G. Georgiou, *Proc. Natl. Acad. Sci. U.S.A.* **96**, 13703 (1999).
4. B. C. Berks, T. Palmer, F. Sargent, *Adv. Microb. Physiol.* **47**, 187 (2003).
5. L. Debarbieux, J. Beckwith, *Proc. Natl. Acad. Sci. U.S.A.* **95**, 10751 (1998).
6. F. E. Dailey, H. C. Berg, *Proc. Natl. Acad. Sci. U.S.A.* **90**, 1043 (1993).
7. E. Mossner, M. Huber-Wunderlich, R. Glockshuber, *Protein Sci.* **7**, 1233 (1998).
8. L. Masip *et al.*, unpublished data.
9. H. Beinert, *Anal. Biochem.* **131**, 373 (1983).
10. S. J. Lippard, J. M. Berg, *Principles of Bioinorganic Chemistry* (University Science Books, Mill Valley, CA, 1994), pp. 115–116.
11. B. A. Lazazzera, H. Beinert, N. Khoroshilova, M. C. Kennedy, P. J. Kiley, *J. Biol. Chem.* **271**, 2762 (1996).
12. J. M. Moulis, V. Davasse, M. P. Golinelli, J. Meyer, I. Quinkal, *J. Biol. Inorg. Chem.* **1**, 2 (1996).
13. V. G. Janolino, H. E. Swaisgood, *J. Biol. Chem.* **250**, 2532 (1975).
14. C. R. Staples *et al.*, *Biochemistry* **35**, 11425 (1996).
15. L. A. Finney, T. V. O'Halloran, *Science* **300**, 931 (2003).
16. A. Holmgren, *J. Biol. Chem.* **254**, 9113 (1979).
17. H. Beinert, R. H. Holm, E. Munck, *Science* **277**, 653 (1997).
18. J. Meyer, *FEBS Lett.* **509**, 1 (2001).
19. D. E. Benson, M. S. Wisz, W. Liu, H. W. Hellinga, *Biochemistry* **37**, 7070 (1998).
20. F. H. Arnold, *Nature* **409**, 253 (2001).
21. S. V. Taylor, P. Kast, D. Hilvert, *Angew. Chem. Int. Ed. Engl.* **40**, 3310 (2001).
22. J. M. Berg, R. H. Holm, *Metal Ions in Biology* **4**, 1 (1982).

23. We thank U. Jakob, P. Kiley, and H. Beinert for many helpful discussions; D. Ballou for help on spectrophotometric measurements; H. Beinert for doing the sulfide assays; T. Huston for performing the ICP–high resolution mass spectroscopy analyses; and T. Palmer and F. Sargent for reading the manuscript. X-ray absorption spectroscopy data were measured at the National Synchrotron Light Source, which is supported by the U.S. Department of Energy (contract no. DE-AC02-98CH10886), at line X9-B, which is supported by the NIH National Center for Research Resources (grant no. P41-RR01633). This work was supported by the Foundation for Research; NSF grant no. BES-220393 (G.G.); and NIH grant nos. GM-55090 (G.G.), GM-57039 and GM-64662 (J.C.A.B.), and GM-38047 (J.E.P.H.). J.F.C. is Charge de Recherches of the Belgian Fonds National de la Recherche Scientifique.

Supporting Online Material

www.sciencemag.org/cgi/content/full/303/5661/1185/DC1
Materials and Methods
SOM Text
Figs. S1 and S2
Table S1
References and Notes

15 October 2003; accepted 6 January 2004

The Structure of a Mycobacterial Outer-Membrane Channel

Michael Faller,[1] Michael Niederweis,[2] Georg E. Schulz[1]*

Mycobacteria have low-permeability outer membranes that render them resistant to most antibiotics. Hydrophilic nutrients can enter by way of transmembrane-channel proteins called porins. An x-ray analysis of the main porin from *Mycobacterium smegmatis*, MspA, revealed a homooctameric goblet-like conformation with a single central channel. This is the first structure of a mycobacterial outer-membrane protein. No structure-related protein was found in the Protein Data Bank. MspA contains two consecutive β barrels with nonpolar outer surfaces that form a ribbon around the porin, which is too narrow to fit the thickness of the mycobacterial outer membrane in contemporary models.

Mycobacteria are of medical importance because members of this genus cause tuberculosis and leprosy (*1*). The treatment of infections is difficult because mycobacteria fortify themselves with a thick impermeable cell envelope (*2*–*6*). One-third (dry mass) of this envelope consists of mycolic acids, which are exceptionally long α-branched β-hydroxy fatty acids of up to 90 carbon atoms (*1*, *7*). The mycolic acids are covalently attached by means of arabinogalactan chains to the peptidoglycan cell wall and form the inner leaflet of an outer membrane (*2*–*5*, *8*). The outer leaflet of this membrane consists of smaller and extractable lipids (*9*). The presence of an outer membrane was corroborated by an x-ray diffraction study showing a quasi-crystalline packing of lipids in the cell walls (*10*) and by freeze fracturing (*3*, *11*). The outer membrane shows low fluidity with phase-transition temperatures as high as 70°C (*12*) and is an extremely efficient permeation barrier protecting the cell from toxic compounds. Based on the lengths of the mycolic acids and their packing properties, as well as on electron micrographs of stained thin sections of mycobacterial cells, present models assume a nonpolar layer thickness of about 90 Å (*3*, *11*). The presence of an outer membrane seems to contradict the assignment of the mycobacteria to the Gram-positive branch based on 16*S* ribosomal RNA sequence comparisons (*13*). However, this inconsistency was recently reconciled by a whole-genome comparison that placed them equidistant to Gram-positive and -negative bacteria (*14*).

For the uptake of small hydrophilic nutrients, mycobacteria have special channels crossing their outer membrane, usually called porins. The porin concentration is low (*15*), which is likely to reduce the vulnerability and the growth rate. These porins were first detected in a cell wall extract of *Mycobacterium chelonae* with the use of lipid bilayer experiments (*16*). It showed a conductance of about 4 nS in 1 M KCl solutions. A similar porin was observed in extracts of *M. smegmatis* cells (*17*) and later purified, characterized, and named MspA (*18*). MspA is the major *M. smegmatis* porin; *M. smegmatis* also contains three other porins designated MspB, MspC, and MspD, which differ from MspA in only 2, 4, and 18 positions, respectively (*19*). No significant sequence similarity between the MspA group and any other protein was detected. The general cylindrical shape of MspA was established by electron microscopy (*15*). Here, we report the atomic structure of this porin, which shows a β structure that differs completely from its counterparts in Gram-negative bacteria (*20*, *21*) and constitutes the first structure of a mycobacterial outer-membrane protein.

For the expression in *Escherichia coli*, we used a designed *E. coli*–adapted gene of MspA without the signal peptide that is known to form an inactive 20-kD monomer and a channel-containing oligomer (*22*). The expression yielded appreciable amounts of monomeric MspA in the cytosol, which was purified by anion exchange chromatography and ammonium sulfate precipitation (*23*). After adding detergent and incubating overnight at a high concentration in the precipitate, monomeric MspA converted to oligomers with a high yield. The oligomers showed a mass greater than 100 kD in SDS–polyacrylamide gel electrophoresis. They formed crystals that were internally disordered and thus useless. Therefore, we produced about a dozen point mutants at predicted surface positions or exchange positions of the isomers MspB, MspC, and MspD (*23*). Among these mutants, $Ala^{96} \rightarrow Arg^{96}$ (A96R) (*24*) formed suitable crystals from fractions at the rise of the oligomer peak in a size exclusion chromatography (fig. S1). These fractions constituted merely 0.5% of the total MspA (*23*). Mutant A96R was

[1]Institut für Organische Chemie und Biochemie, Albert-Ludwigs-Universität, Albertstrasse 21, 79104 Freiburg im Breisgau, Germany. [2]Lehrstuhl für Mikrobiologie, Friedrich-Alexander-Universität Erlangen-Nürnberg, Staudtstrasse 5, 91058 Erlangen, Germany.

*To whom correspondence should be addressed. E-mail: schulz@bio.chemie.uni-freiburg.de

named MspA(R) and used in all further analyses. For phasing, we mutated Leu[88] to a second methionine resulting in double mutant MspA(RM), which was grown in a methionine-auxotrophic *E. coli* strain in the presence of selenomethionine (*23*) and prepared as well as crystallized in the same manner as MspA(R). Using synchrotron radiation at the Se-K absorption edge, we derived phases at 3.0 Å resolution (*23*). The respective electron density map revealed two MspA monomers arranged around a crystallographic fourfold axis forming an octameric complex with an eightfold rotation axis. Using a 2.5 Å resolution data set of MspA(R) (table S1), we subsequently refined the protein model to high accuracy (table S2).

The structure of porin MspA is illustrated in Fig. 1. The polypeptide forms a tightly interconnected octamer with eightfold rotation symmetry that resembles a goblet and contains a central channel. Each subunit consists of a 134-residue globular domain building up the thick rim of the goblet, and a 50-residue loop forms the stem and the base. The sequence and the secondary structure are given in Fig. 2A. No similar structure was found in the Protein Data Bank. The rim domain is a sandwich of two four-stranded completely antiparallel β sheets (Fig. 2B). The interface area between two rim domains is as large as 1050 Å^2 and contains a short β-sheet connection between β10 and the neighboring β12 (Fig. 2B).

The 50-residue loop participates in two 16-stranded conventional β barrels (*21*) that have essentially circular cross-sections as a result of the eightfold rotation symmetry. The longer β barrel forms the goblet stem. It has a shear number (*25*) of 32, giving rise to a β-strand tilting angle of 56° against the membrane normal, which is even larger than the 51° of the composite β barrel of TolC (*21*, *26*). The large tilting angle causes a wide barrel with a diameter of 40 Å (Cα atoms). The base of the goblet contains a second, short 16-stranded β barrel that forms a channel constriction, also called a pore eyelet, with a diameter of 28 Å (Cα atoms). This barrel has a shear number of 16 and a tilting angle of 37°, similar to that of the composite β barrel of α-hemolysin (*27*). The change of the shear number from 32 to 16 is a previously unobserved feature. Such a change is an elegant way of reducing the β-barrel diameter without changing the number of strands (*25*).

The height of the goblet is 96 Å and the largest outer diameter of the octamer is 88 Å (Fig. 3A). These dimensions are similar to the values derived from electron micrographs (*15*). The outer diameter of the 16-stranded β barrel is 49 Å. The channel diameter varies between 48 and 10 Å at the pore eyelet (Fig. 3A). The orientation of the porin in the outer mycobacterial membrane was derived from a mouse antiserum raised against a surface peptide on the goblet rim (*23*). This peptide is marked in Fig. 1 and specified in Fig. 2A. Because the antiserum bound to whole *M. smegmatis* cells (*23*), the rim is the external end of the porin.

The surface of the central channel is generally polar, except for a nonpolar ring on the external side of the pore eyelet (Fig. 4A). The eyelet is fully defined by the carboxylates of Asp[90] and Asp[91] (Fig. 4B) that cause a rather strong electric field diminishing the permeability for nonpolar solutes. None of the 380 water molecules associated with the goblet is in a noteworthy position. The calculated electric conductance for a pore of this size and shape in a 1 M KCl solution (specific conductivity 1.13 S cm^{-1}) is 5.1 nS if the bulk solvent were considered to begin 3.0 Å outside the surfacial non-hydrogen atoms and if all interactions with charges on the protein surface were neglected. Because the calculated conductance is only 10% higher than the measured value of 4.6 nS (*18*), we conclude that the MspA pore behaves electrically essentially like a rod of conducting bulk solvent. In contrast, the porin from *Rhodobacter capsulatus* contains three channels that would form a shorter and wider pore if

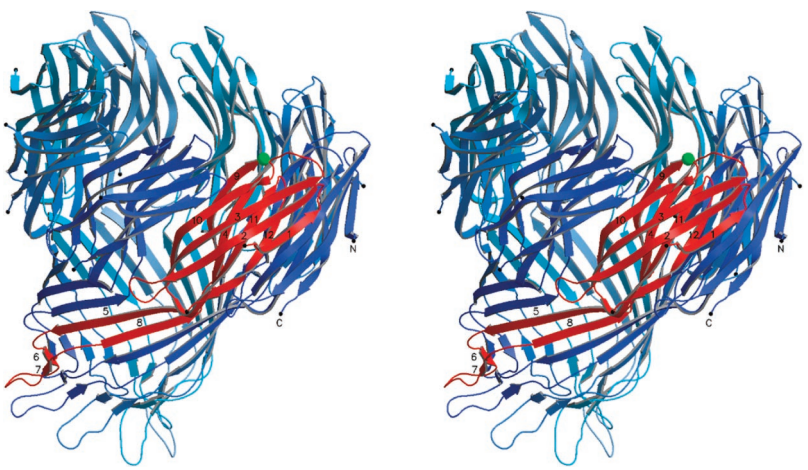

Fig. 1. Stereoview of a ribbon plot of the octameric MspA porin from *M. smegmatis*, which we describe as a goblet consisting of a thick rim at the top, a stem consisting of the wide β barrel, and a base at the bottom. One of the subunits is emphasized (red) and shows the β strand numbers. The outermost residue Ser[136] of the peptide segment used for raising a mouse antiserum (*23*) is marked by a green ball. The β barrel at the goblet stem contains 16 strands with a shear number (*25*) as high as 32. The second β barrel at the goblet base has a shear number of 16, giving rise to a much smaller diameter and thus to a constriction (*25*).

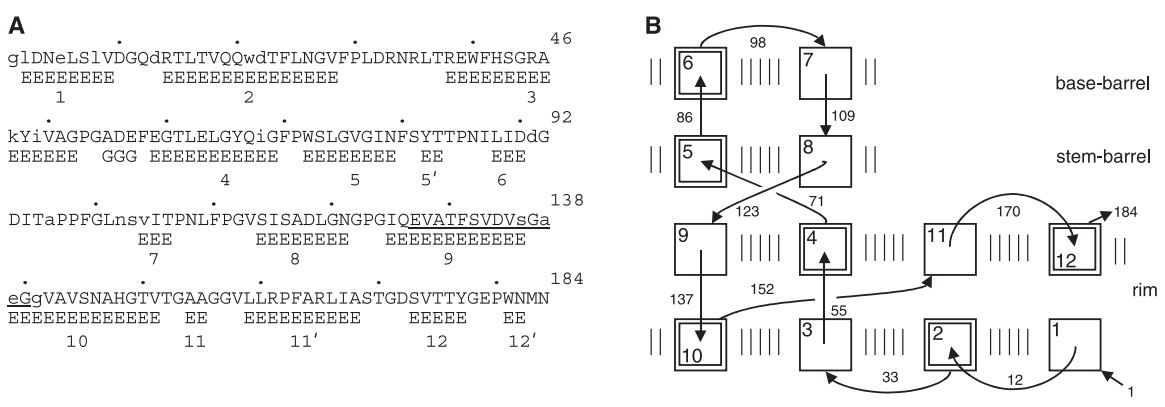

Fig. 2. Sequence, secondary structure, and topology of the MspA porin. (**A**) Sequence (upper line) and secondary structure assignment (lower line; E, β strand; G, 3_{10} helix). The 19 exchange positions of the three known homologs MspB, MspC, and MspD (*19*) are marked by lowercase letters. The peptide segment used for raising a mouse antiserum (*23*) is underlined. Strands β5, β11, and β12 are split by β bulges. (**B**) Topology: 8 of the 12 β strands assemble in the two sandwiched four-stranded β sheets forming the goblet rim domain shown in Fig. 1. The contact between rim domains extends the β sheets to neighboring subunits as indicated by the hydrogen bond markings at strands β10 and β12. Strands β5 and β8 form the composite β barrel of the goblet stem and strands β6 and β7 form the composite β barrel at the goblet base. Residue numbers in loops are given.

the three cross-sectional areas were added up and converted to a hypothetical single circular cross-section (Fig. 3B). Calculating the conduction of this hypothetical channel under the same assumption as used for MspA resulted in 13 nS, which is four times the experimental value of 3.3 nS (*28*). We therefore conclude that a crooked narrow geometry reduces the ionic conductance appreciably below that of a straight smooth channel with equivalent cross-sectional areas.

The outer surface of the goblet shows a clear subdivision into the polar surface of the globular rim domains and the nonpolar surface of the goblet's stem and base. The border is clearly marked by the two rings of Arg^{35} and Arg^{38} side chains that point into the environment (Fig. 3A). These arginines are charged and are likely to bind to phosphoryl groups of lipids in the external leaflet of the outer membrane. This nonpolar surface forms a ribbon around the porin, which confirms the very existence of an outer membrane in mycobacteria. The width of the nonpolar ribbon is 37 Å, which is wider than the corresponding 26 Å of the porins of Gram-negative bacteria (*20*), an example of which is depicted in Fig. 3B. The nonpolar ribbon around MspA contains some aromatic side chains, but these are not arranged like the two girdles lining the ribbon in Gram-negative bacteria, which was interpreted as contacting the two polar/nonpolar-interface layers of the outer membrane (*20*).

Therefore, the lipidic layer of the mycobacterial outer membrane probably has a thickness of not more than 37 Å, which is in stark contrast to the present outer-membrane models suggesting about 90 Å. In principle, the 90 Å can nearly be reached by two consecutive goblets associated base to base. Such a contact exists in the crystals, where it is tightened by eight hydrogen bonds introduced by the mutation A96R. Because none of our screenings with wild-type MspA or other mutants yielded any ordered crystals diffracting x-rays to better than 10 Å resolution, however, the precision of this base-to-base packing contact obviously depends on the added arginine of A96R, indicating that the contact is not natural. Also, no such contact was found under the electron microscope (*15*). Moreover, position 96 and others at the goblet base are targets for the rare natural exchanges (Fig. 2A), demonstrating that they are functionally less important than, for instance, the large number of residues facing the membrane. These facts render a natural base-to-base association very unlikely. In conclusion, the mycobacterial outer-membrane models should be revisited. It is conceivable that the mycolic acids do not extend perpendicularly to the membrane but fold back and/or intertwine excessively, forming a layer that is much thinner but still very strong.

Functional information on a novel structure can usually be deduced from related amino acid sequences. Unfortunately, MspA has only the three closely related isomers with 19 exchange positions (Fig. 2A). Among them (*19*), MspB shows exchanges A138P and E139A in a loop at the top of the goblet rim: Proline fortifies the loop and alanine removes a negative charge at the external end changing the antigenic properties. MspC has A96G and N102E in addition to those of MspB: Glycine is at the tip of the long loop pointing into the periplasm (bottom of Fig.

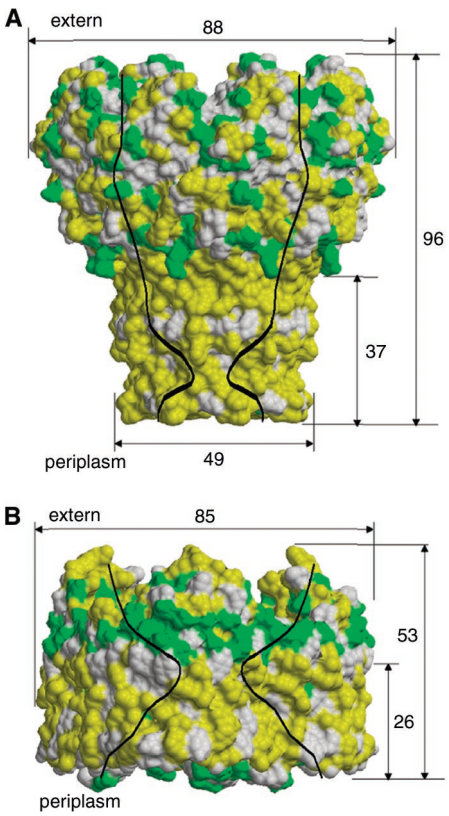

Fig. 3. Hydrophobicity of the outer surfaces (green, polar; yellow, nonpolar) of two porins depicted at the same scale with dimension given in Å. (**A**) Mycobacterial MspA showing the channel lining in black. Because of the eightfold rotation symmetry, the entire channel is nearly circular. The nonpolar surface ribbon extends over 37 Å from the Arg^{35} and Arg^{38} side chains (green) to the bottom. (**B**) The major porin of *R. capsulatus* as a representative for Gram-negative bacteria (*20*, *21*). At its external end, the porin contains a single channel that splits into three channels at the periplasmic end. The channel cross-sections deviate appreciably from circles. The black lines indicate the size of a hypothetical circular single channel with the same cross-sectional area as the three natural channels at each height.

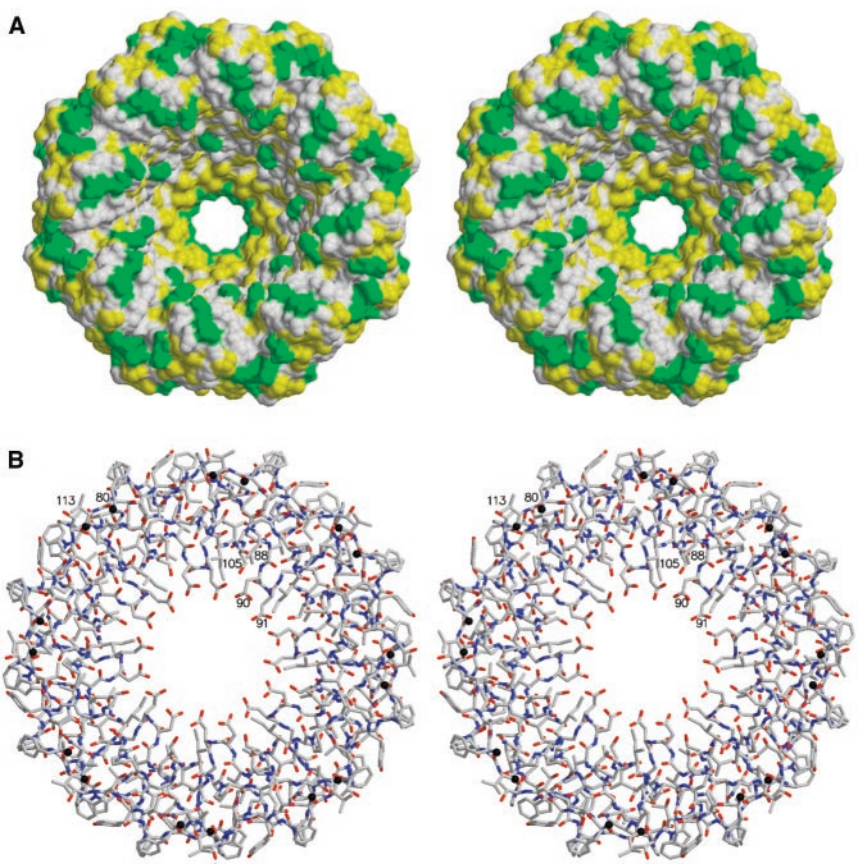

Fig. 4. Stereoview from the external medium into the MspA channel. The image in (B) is enlarged by a factor of 1.9 as compared with (A). (**A**) View from the external compartment into the pore of a surface model showing the shape and the polar (green) and nonpolar (yellow) surfaces. (**B**) The same view at the atomic level showing the two rings of aspartates at the eyelet and a nonpolar ring consisting of leucines and isoleucines on the external side of the eyelet. For clarity, the peptide is truncated within the goblet stem (black dots). Some residues from one subunit are labeled.

1), rendering this loop more mobile; glutamate brings a further negative charge into the channel on the periplasmic side of the eyelet and may therefore change the permeation properties slightly. The exchange D91G of MspD removes the side chain defining the pore eyelet diameter (Fig. 4B) and should therefore increase the permeability decisively. N102D of MspD introduces a negative charge on the periplasmic side of the eyelet similar to an exchange in MspC. S103T and V104I should improve the stability of the chain at the goblet base, and the glutamine of A96Q projects into the periplasm. I68V is in the nonpolar core of the rim domain, whereas L8V and G141A strengthen the interface between these domains. Exchanges G1A, L2V, E5Q, W21A, D22E, K47T, and I49H are on the outer-domain surface about 20 Å below the goblet rim, varying the charge distribution and thus the expected interaction with components of the outer leaflet of the outer membrane. In particular, the removal of the protruding tryptophan should reduce the sugar-binding capacity (*29*). S136K and E139K on the rim change the antigenic properties of MspD compared with the other isomers. The interactions of MspA with the outer membrane may be analyzed in the crystal because the outer surface of four of the eight rim domains is freely accessible so that soaking experiments with membrane constituents are feasible.

Among the mycobacteria, *Mycobacterium tuberculosis* is carried by about two billion people and causes a higher death rate than any other infectious agent (*30*). *M. tuberculosis* and its close relative *Mycobacterium bovis* have porins with conductances of about 0.8 and 4 nS in 1 M KCl solutions that were detected in detergent extracts but could not be further characterized (*31*, *32*). These porins are thought to be crucial for drug efficacy because the three important drugs—isoniazide, ethambutol, and pyrazinamide—are small polar molecules (*6*) that, for instance, can easily permeate the channel constriction of MspA (Fig. 4B). Because porin sequences are highly variable (*33*), the lack of sequence similarity does not exclude a structural relationship to MspA. Therefore, it seems worthwhile to perform an MspA-based structure knowledge-directed search to identify the large porin in the *M. tuberculosis* genome. Any detected gene may then be expressed, purified, and crystallized like MspA.

References and Notes

1. N. Rastogi, E. Legrand, C. Sola, *Rev. Sci. Tech.* **20**, 21 (2001).
2. D. E. Minnikin, *Res. Microbiol.* **142**, 423 (1991).
3. P. J. Brennan, H. Nikaido, *Annu. Rev. Biochem.* **64**, 29 (1995).
4. C. E. Barry III *et al.*, *Prog. Lipid Res.* **37**, 143 (1998).
5. M. Daffé, P. Draper, *Adv. Microb. Physiol.* **39**, 131 (1998).
6. P. A. Lambert, *J. Appl. Microbiol.* **92**, 46S (2002).
7. M. Watanabe, Y. Aoyagi, M. Ridell, D. E. Minnikin, *Microbiology* **147**, 1825 (2001).
8. B. A. Dmitriev, S. Ehlers, E. T. Rietschel, P. J. Brennan, *Int. J. Med. Microbiol.* **290**, 251 (2000).
9. M. Jackson, D. C. Crick, P. J. Brennan, *J. Biol. Chem.* **275**, 30092 (2000).
10. H. Nikaido, S. H. Kim, E. Y. Rosenberg, *Mol. Microbiol.* **8**, 1025 (1993).
11. T. R. Paul, T. J. Beveridge, *J. Bacteriol.* **174**, 6508 (1992).
12. J. Liu, E. Y. Rosenberg, H. Nikaido, *Proc. Natl. Acad. Sci. U.S.A.* **92**, 11254 (1995).
13. C. Pitulle, M. Dorsch, J. Kazda, J. Wolters, E. Stackebrandt, *Int. J. Syst. Bacteriol.* **42**, 337 (1992).
14. L. M. Fu, C. S. Fu-Liu, *Tuberculosis* **82**, 85 (2002).
15. H. Engelhardt, C. Heinz, M. Niederweis, *J. Biol. Chem.* **277**, 37567 (2002).
16. J. Trias, V. Jarlier, R. Benz, *Science* **258**, 1479 (1992).
17. J. Trias, R. Benz, *Mol. Microbiol.* **14**, 283 (1994).
18. M. Niederweis *et al.*, *Mol. Microbiol.* **33**, 933 (1999).
19. C. Stahl *et al.*, *Mol. Microbiol.* **40**, 451 (2001).
20. M. S. Weiss *et al.*, *FEBS Lett.* **280**, 379 (1990).
21. G. E. Schulz, *Biochim. Biophys. Acta* **1565**, 308 (2002).
22. C. Heinz, S. Karosi, M. Niederweis, *J. Chromatogr. B. Anal. Technol. Biomed Life Sci.* **790**, 337 (2003).
23. Experimental data are available as supporting material on *Science* Online.
24. Single-letter abbreviations for the amino acid residues are as follows: A, Ala; C, Cys; D, Asp; E, Glu; F, Phe; G, Gly; H, His; I, Ile; K, Lys; L, Leu; M, Met; N, Asn; P, Pro; Q, Gln; R, Arg; S, Ser; T, Thr; V, Val; W, Trp; and Y, Tyr.
25. The shear number S of a β barrel is derived by running from a given residue of a given β strand along the hydrogen bonds once around the barrel and counting the offset number of residues on return. For a regular 16-stranded β barrel, the square of the circumference is $(4900 + 11S^2)$ Å^2, showing the dependence of the diameter on the shear number (*21*).
26. V. Koronakis, A. Scharff, E. Koronakis, B. Luisi, C. Hughes, *Nature* **405**, 914 (2000).
27. L. Song *et al.*, *Science* **274**, 1859 (1996).
28. R. Benz, K. Bauer, *Eur. J. Biochem.* **176**, 1 (1988).
29. J. E. W. Meyer, G. E. Schulz, *Protein Sci.* **6**, 1084 (1997).
30. D. Bleed, C. Watt, C. Dye, "Global tuberculosis control" (WHO Report, Geneva, 2001).
31. B. Kartmann, S. Stenger, M. Niederweis, *J. Bacteriol.* **181**, 6543, Corrigendum p. 7650 (1999).
32. T. Lichtinger *et al.*, *FEBS Lett.* **454**, 349 (1999).
33. E. Schiltz, A. Kreusch, U. Nestel, G. E. Schulz, *Eur. J. Biochem.* **199**, 587 (1991).

34. The coordinates and structure factors are deposited in the Protein Data Bank under accession code 1UUN. We thank the teams of the European Molecular Biology Laboratory (EMBL)–outstation at Deutsches Elektronen-synchrotron (DESY) (Hamburg) and of the Swiss Light Source (SLS) (Villigen) for their help in data collection; and D. Frey, C. Heinz, P. Hülsmann, D. Kloer, and M. Ziegler for help at various stages of the analysis. Supported by the Deutsche Forschungsgemeinschaft under SFB-388 and Ni-412.

Supporting Online Material

www.sciencemag.org/cgi/content/full/303/5661/1189/DC1
SOM Text
Fig. S1
Tables S1 and S2
References

1 December 2003; accepted 12 January 2004

Use of CD134 As a Primary Receptor by the Feline Immunodeficiency Virus

Masayuki Shimojima,[1]* Takayuki Miyazawa,[2,3]* Yasuhiro Ikeda,[4] Elizabeth L. McMonagle,[5] Hayley Haining,[5] Hiroomi Akashi,[1] Yasuhiro Takeuchi,[4] Margaret J. Hosie,[5] Brian J. Willett[5]†

Feline immunodeficiency virus (FIV) induces a disease similar to acquired immunodeficiency syndrome (AIDS) in cats, yet in contrast to human immunodeficiency virus (HIV), CD4 is not the viral receptor. We identified a primary receptor for FIV as CD134 (OX40), a T cell activation antigen and costimulatory molecule. CD134 expression promotes viral binding and renders cells permissive for viral entry, productive infection, and syncytium formation. Infection is CXCR4-dependent, analogous to infection with X4 strains of HIV. Thus, despite the evolutionary divergence of the feline and human lentiviruses, both viruses use receptors that target the virus to a subset of cells that are pivotal to the acquired immune response.

The primary event in the process of viral entry into a target cell is the interaction between the virus and its cellular receptor, and the specificity of this interaction determines both viral cell tropism and pathogenicity. For the primate lentiviruses, the viral receptor is CD4, targeting the virus to helper T cells, resulting in their depletion and the eventual development of acquired immunodeficiency syndrome (AIDS) (*1*). However, CD4 expression alone is insufficient to confer susceptibility to infection with human immunodeficiency virus (HIV), which also depends on the expression of coreceptors, principally the chemokine receptors CXCR4 and CCR5 (*2*). The virus attaches via a high-affinity interaction with CD4, resulting in a conformational change in the envelope glycoprotein (Env) and exposing the binding site for the chemokine receptor (*3*). This then triggers a further conformational change that exposes the fusion domain of the viral transmembrane protein gp41 and enables fusion of the viral and cellular membranes (*4*).

[1]Department of Veterinary Microbiology, Graduate School of Agricultural and Life Sciences, University of Tokyo, 1-1-1 Yayoi, Bunkyo-ku, Tokyo 113-8657, Japan. [2]Department of Veterinary Public Health, Obihiro University of Agriculture and Veterinary Medicine, Inada-cho, Obihiro, Hokkaido 080-8555, Japan. [3]Host and Defense, PRESTO, Japan Science and Technology Agency, 4-1-8 Honcho, Kawaguchi, Saitama 332-0012, Japan. [4]Department of Immunology and Molecular Pathology, Windeyer Institute of Medical Sciences, University College London, London W1T 4JF, UK. [5]Retrovirus Research Laboratory, Institute of Comparative Medicine, University of Glasgow, Glasgow G61 1QH, UK.

*These authors contributed equally to this work
†To whom correspondence should be addressed. E-mail: b.willett@vet.gla.ac.uk